CONTRIBUTION FROM THE CHEMICAL ENGINEERING DIVISION
ARGONNE NATIONAL LABORATORY, ARGONNE, ILLINOIS

Studies of Lithium Hydride Systems. I. Solid–Liquid Equilibrium in the Lithium Chloride–Lithium Hydride System[1]

BY CARL E. JOHNSON, SCOTT E. WOOD, AND CARL E. CROUTHAMEL

Received May 18, 1964

Thermal analysis has been used to determine the temperature–composition solid–liquid equilibrium diagram for the lithium hydride–lithium chloride binary mixture. A eutectic composition of 34.0 mole % lithium hydride was observed, melting at 495.6°. No formation of solid solutions was observed. Calculations have been made of the chemical potential for each component in the composition region for their solid–liquid equilibrium. The system exhibits positive deviations from ideal behavior. The positive deviations in the dilute solutions of lithium chloride in lithium hydride might be interpreted in terms of dimerization of the lithium chloride.

Introduction

Increased interest in the chemistry of lithium hydride has resulted from its anticipated use in fluids which will function in direct energy conversion devices.[2] A knowledge of the solid–liquid equilibrium phase diagram for the LiCl–LiH system is necessary in the design and operation of such a device. The data have been used to calculate some of the thermodynamic properties of lithium hydride in the molten salt mixture.

Experimental

Apparatus.—As the whole of the experimental program involved working with metals and salts which were extremely sensitive to the chemically active gases, it was deemed important to obtain an inert atmosphere of very high purity. This problem concerned not only the absolute purity of the original charge of blanket gas but also one of maintaining the purity of the box atmosphere in the face of continuing contamination. These conditions were met by the development[3] of a helium gas purification unit which continuously circulates purified helium through the box. Impurity levels during normal operation in the box were below 5 p.p.m. for both oxygen and nitrogen and below 1 p.p.m. for water.

The thermal analysis apparatus was patterned after that described by Smith.[4] The essential parts of the apparatus are shown in Fig. 1. The furnace tube was connected directly to the inert atmosphere box so that reactive salts and metals could be weighed and introduced into the sample holder without contamination. The sample was placed in a type 347 stainless steel crucible (1 in. diameter × 1.5 in. high × 0.015 in. wall and bottom) which in turn was placed in a firebrick container of low thermal conductivity. The firebrick was enclosed in type 347 stainless steel. The tip of the central thermowell has three circular heat-conducting fins 0.010 in. thick which extend to the wall of the sample cup.

In all experiments the temperature of the furnace was maintained at a constant differential amount above or below the sample temperature. This was achieved by using a separate differential thermocouple with its junctions inside and outside the sample container wall to regulate the temperature difference. The output of this differential thermocouple operated a differential d.c. amplifier which controlled the heating and cooling rate of the sample. The versatility in adjustment of this amplifier allowed heating and cooling rates to be changed from 0.2 to 10°/min., thereby controlling very closely the heat flow into and out of the sample.

The differential d.c. amplifier activated a proportionating controller which in turn operated a magnetic amplifier. The power to the furnace surrounding the sample was supplied through a saturable core reactor controlled by the magnetic amplifier.

An adjustable span, adjustable suppression recording potentiometer was used to record the temperature of the melt. Temperatures were measured with calibrated platinum–platinum 10% rhodium thermocouples, which were calibrated against the melting points of N.B.S. pure Zn (m.p. 419.5°) and N.B.S. pure Al (m.p. 660.0°). The accuracy of the absolute value of the temperature was estimated to be ±0.3°.

Materials.—The lithium metal was obtained from Foote Mineral Co. of Philadelphia, Pa. The impurity analysis supplied by the Foote Mineral Co. was 0.003% Na, 0.003% K, 0.003% N_2, and 0.003% Cl_2. Before use, the metal was trimmed free of any surface oxide or nitride coating.

Commercial hydrogen gas was purified before use by passage through a silver–palladium alloy[5] held at 400°.

Lithium hydride was prepared by contacting liquid lithium metal at 750° with purified hydrogen at 1 atm. for 12 hr. The material was cooled in hydrogen and transferred immediately under vacuum to the high purity helium atmosphere box. Samples of freshly prepared lithium hydride were dissolved in alcohol–water mixtures and titrated with standardized hydrochloric acid. Analyses indicated greater than 99.8% lithium hydride in the material. The melting point of the lithium hydride was 685.9°. This is 2.1° lower than the 688° reported by Messer, *et al.*,[6] in their original publication but compares favorably with the 686.4° given in their subsequent report.[7]

Reagent grade lithium chloride was purified with chlorine gas using the method of Maricle and Hume.[8] The lithium chloride melting point was 606.8°.

Method.—In all experiments crystalline lithium hydride and lithium chloride were weighed (total weight about 23 g.) into the crucible and the whole (Fig. 1) was introduced into the furnace well connected to the floor of the helium atmosphere box. Before heating the sample, the furnace well was sealed from the box atmosphere, evacuated, and filled with purified hydrogen to about 800 mm. pressure. The sample was then heated to melt the pure components and held in the liquid state for 1 hr. The temperature was then decreased and the first break in the cooling curve was observed. This operation was repeated until the location of the first break was consistent, after which complete cooling and

(1) This work was performed under the auspices of the U. S. Atomic Energy Commission.
(2) R. C. Werner and T. A. Ciarlariello, U. N. Geneva Conference 35/GEN/14 (1961).
(3) M. S. Foster, C. E. Johnson, and C. E. Crouthamel, Report USAEC-ANL-6652 (Dec., 1962).
(4) C. S. Smith, *Trans. AIME*, **137**, 236 (1940).
(5) Instrument purchased from Englehard Industries, Inc., Newark, N. J.
(6) C. E. Messer, E. B. Damon, P. C. Maybury, J. Mellor, and R. A. Searles, *J. Phys. Chem.*, **62**, 220 (1958).
(7) C. E. Messer and J. Mellor, *ibid.*, **64**, 503 (1960).
(8) D. L. Maricle and D. N. Hume, *J. Electrochem. Soc.*, **107**, 354 (1960).

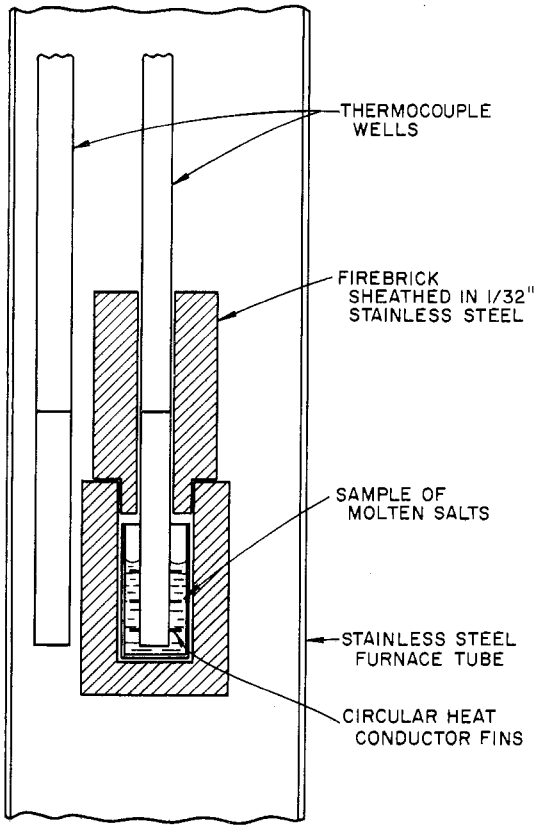

Fig. 1.—Thermal analysis sample assembly.

heating curves were determined. This procedure was followed to ensure complete mixing of the components in the system.

The sample composition was calculated from the weights of the pure materials. However, periodic checks were made by chemical analysis for the composition of the fused salt mixture.

In the experiments the solid–liquid equilibrium breaks in the cooling and heating curves were observed under pure hydrogen at 1.50 ± 0.50 atm. The pure hydrogen atmosphere was effective in preventing any appreciable decomposition of the lithium hydride component into lithium metal and hydrogen gas. This was accomplished even with pure lithium hydride at its melting point. Evidence for this was the ability to obtain a consistently reproducible melting point on the same sample of pure lithium hydride at 1–3 atm. hydrogen pressure. Also, the solid–liquid equilibrium temperature in the lithium hydride rich portion of the diagram was constant with repeated heating and cooling curve observations and was not sensitive to hydrogen pressure variations of 1–2 atm.

Results and Discussion

Temperature composition data for the lithium hydride–lithium chloride system were obtained over the composition range of 0–100% lithium hydride. These data are given in Fig. 2 and the first two columns of Table I. A eutectic composition of 34.0 mole % lithium hydride was observed, the eutectic melting at 495.6°. The eutectic melting point was constant (±1°) across the diagram. Formation of solid solution was not observed in either thermal analysis of the solid–liquid equilibrium or X-ray diffraction analysis of the solids. Initial experimental work on the lithium chloride side encountered difficulty in defining the correct solid–liquid equilibrium temperatures. Modification of the central thermowell to include three thermal-conducting fins corrected this problem.[9]

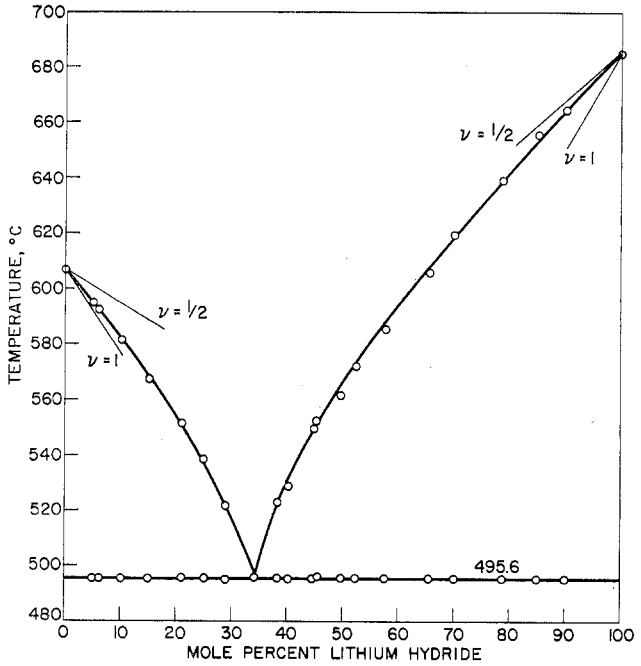

Fig. 2.—LiH–LiCl solid–liquid equilibrium—under 1 atm. of H_2(g).

TABLE I

THERMODYNAMIC PROPERTIES OF THE SYSTEM LiH–LiCl

LiH, mole %	T_e, °K.	μ^M_{LiCl}, cal./mole	μ^M_{LiH}, cal./mole	μ^E_{LiCl}, cal./mole	μ^E_{LiH}, cal./mole
0.0	880.0	...		...	
5.0	868.2	−64.3		24.2	
6.1	865.6	−76.8		31.5	
10.1	854.7	−135		45.4	
15.1	840.7	−205		68.7	
21.0	824.8	−295		91.2	
24.9	811.7	−348		114	
28.9	794.9	−454		84.9	
34.0	768.8	−590	−1089	44.3	558
38.2	796.4		−927		597
40.1	802.3		−893		565
44.7	822.7		−773		551
45.1	825.6		−755		543
49.5	834.8		−701		464
52.2	845.5		−648		443
57.6	859.0		−562		380
65.4	889.0		−447		295
69.8	892.9		−368		269
78.6	912.7		−257		179
85.2	929.1		−164		132
90.1	938.3		−114		79.8
100.0	959.3		...		...

The data are represented in Fig. 3, in which log x is given as a function of the reciprocal of the absolute temperature. The upper curve is obtained from the lithium chloride side of the phase diagram and the lower from the lithium hydride side. The dotted lines give the ideal solubility of the solid component in the solution. The points represent the experimental data. It is evident that the lines formed by the points pass through the melting point of the pure component at unit mole

(9) C. E. Johnson, C. E. Crouthamel, and S. E. Wood, *Nature*, **201**, 293 (1964).

fraction. A problem is apparent at the eutectic temperature ($10^3/T = 1.30$). The point for each component apparently does not lie on the smooth curves formed by the two sets of data points; neither is it possible to adjust the eutectic temperature or the eutectic composition within reasonable limits to bring the points onto the smooth curves. Experimental analyses were made defining the eutectic composition. It is possible that a new phase appears in the immediate vicinity of the eutectic point similar to that observed in the sodium carbonate–lithium carbonate system.[10] However, such a new phase has not been observed by X-ray diffraction analyses of the solid phases at and near the eutectic composition.

In the thermodynamic analysis of these data, with no experimental evidence for the presence of solid solutions, it was assumed that only the pure solid component was precipitating from the mixture. For such a system the change of the chemical potential on mixing, $\Delta\mu^M$, for the component in solution which is in equilibrium with the pure solid is calculated by use of the equation

$$\Delta\mu^M{}_1(x_2T_e) = \Delta\tilde{H}_f\left(\frac{T_e - T_{m_1}}{T_{m_1}}\right) + T_e\int_{T_{m_1}}^{T_e}\frac{dT}{T^2}\int_{T_{m_1}}^{T}(\tilde{C}_{p_1}^{(l)} - \tilde{C}_{p_1}^{(s)})\,dT \quad (1)$$

In this equation, $\Delta\tilde{H}_f$ is the molar change of enthalpy of the pure component on melting at its melting point, T_m. T_e is the equilibrium temperature of the two-phase system. The standard state of the component in solution is chosen to be the pure supercooled liquid at the equilibrium temperature and 1 atm. It has been assumed that a variation in pressure of ± 0.5 atm. will not affect appreciably the equilibrium temperatures, T_e, of the two-phase system.

The heat capacity and heat of fusion data needed for lithium chloride were obtained from JANAF tables.[11] Vogt[12] has tabulated similar data for lithium hydride. The values of the heat capacity in cal. deg.$^{-1}$ mole^{-1} used in the calculations are

$$\text{LiH}\begin{cases}\tilde{C}_p^{(s)} = 7.26 + 11.3 \times 10^{-3}T \\ \tilde{C}_p^{(l)} = 15.8 - 1.01 \times 10^{-3}T\end{cases}$$

$$\text{LiCl}\begin{cases}\tilde{C}_p^{(s)} = 10.4 + 4.95 \times 10^{-3}T - 3.98 \times 10^4/T^2 \\ \tilde{C}_p^{(l)} = 17.5 - 2.26 \times 10^{-3}T\end{cases}$$

The values of the molar enthalpy change of the pure components on fusion in kcal. mole^{-1} used in the calculations are: LiH, $\Delta\tilde{H}_f = 5.24$; LiCl, $\Delta\tilde{H}_f = 4.74$.

It is convenient to express the thermodynamic behavior of the system in terms of the excess chemical potentials defined by the equations

$$\Delta\mu^E{}_1(x_2) = \Delta\mu^M{}_1 - RT_e \ln(1 - x_2) = RT \ln \gamma_1 \quad (2)$$

$$\Delta\mu^E{}_2(x_2) = \Delta\mu^M{}_2 - RT_e \ln x_2 = RT \ln \gamma_2 \quad (3)$$

(10) E. J. Cairns and D. I. MacDonald, *Nature*, **194**, 441 (1962).
(11) JANAF Thermochemical Tables, Dow Chemical Company, Midland, Mich., 1962.
(12) J. W. Vogt, TAPCO Report NP-11888.

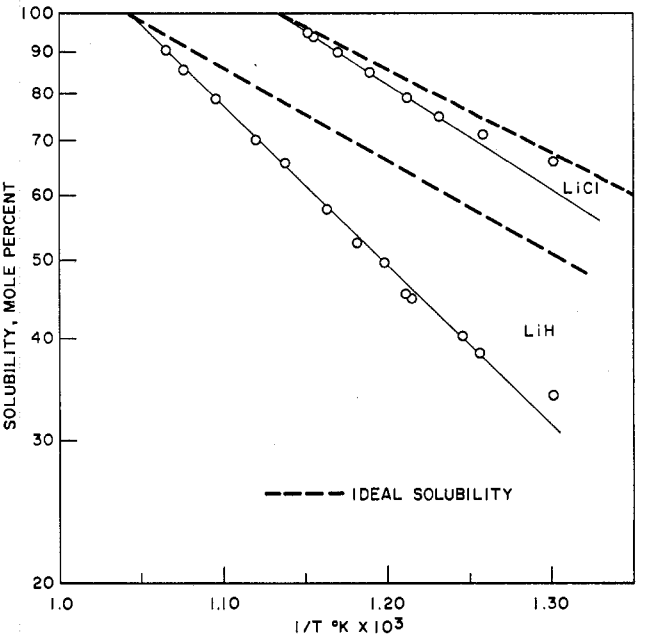

Fig. 3.—Solubility *vs.* temperature for the LiH–LiCl system.

With the use of these equations and the solid–liquid equilibrium data, calculations have been made of the chemical potentials for each component over the composition ranges in which these components precipitate from solution. The values of $\Delta\mu^M$ calculated from eq. 1–3 are given in the third and fourth columns of Table I for lithium chloride and lithium hydride, respectively. The corresponding values of $\Delta\mu^E$ are given in the fifth and sixth columns.

The smoothing of the excess chemical potentials given in Table I and the study of the thermodynamic consistency of the data cannot be developed without simplifying assumptions. It is expected that the molar thermodynamic functions of the liquid phase can be expressed by the same function over the entire range of composition. However, only the excess chemical potential of one of the components along the saturation curve has been determined on either side of the diagram at an assumed constant pressure. As stated previously the effect of pressure is assumed to be zero. The complete Gibbs–Duhem equation for the saturated liquid phase at constant pressure is

$$\left(\frac{\partial\Delta\mu^E{}_2}{\partial x_1}\right)_P = -\frac{x_1}{x_2}\left[\left(\frac{\partial\Delta\mu^E{}_1}{\partial x_1}\right)_P + \Delta\tilde{S}^E\left(\frac{\partial T}{\partial \ln x_1}\right)_P\right] \quad (4)$$

where $\Delta\tilde{S}^E$ is the excess molal entropy of the solution. Without knowledge of $\Delta\tilde{S}^E$, the use of this equation requires the assumption that $\Delta\tilde{S}^E$ be zero. Such an assumption makes the excess Gibbs free energy independent of temperature and equal to the change of enthalpy on mixing. However, the use of eq. 4 in order to study the thermodynamic consistency of the data requires the extrapolation of $\Delta\mu^E{}_1$ as a function of x_1 into the region where no measurements can be made.

To overcome this difficulty $\Delta\tilde{G}^E$, the excess molal free

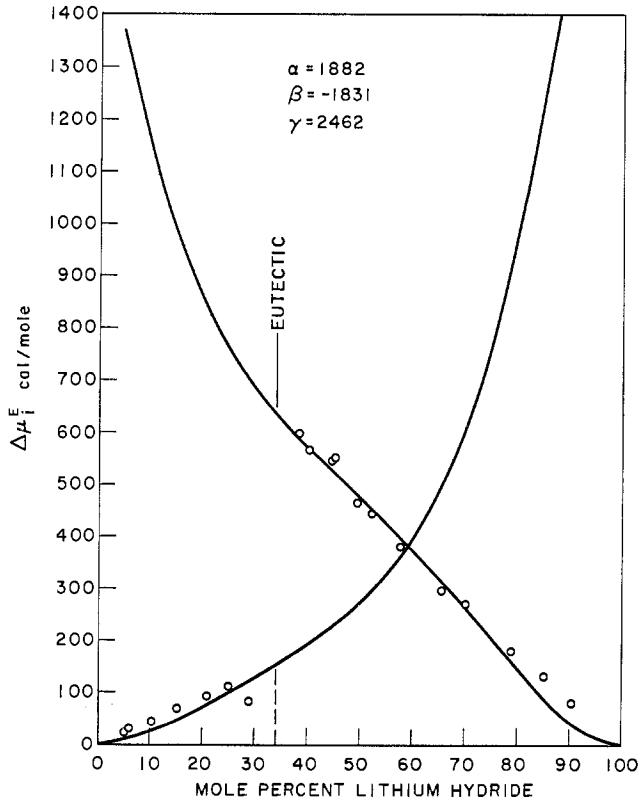

Fig. 4.—Excess chemical potentials of LiH and LiCl.

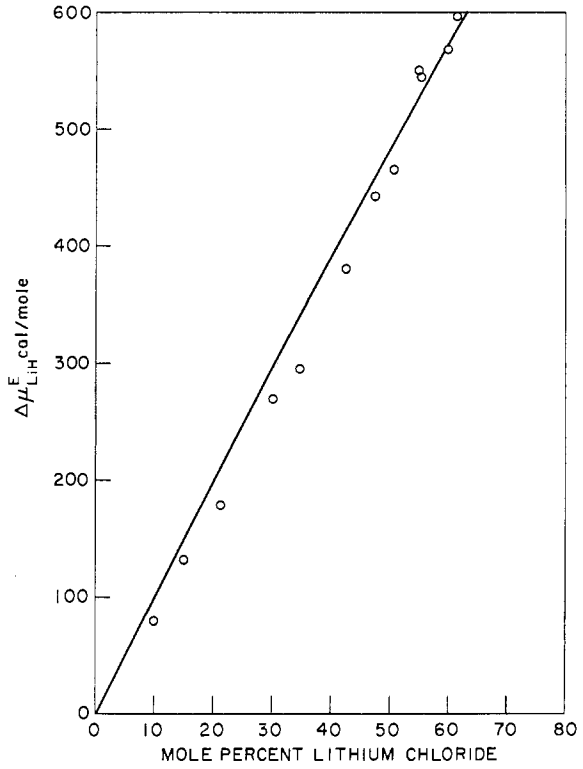

Fig. 5.—Comparison of experimental data for $\Delta\mu^E_{LiH}$ with values calculated assuming Li_2Cl_2 and LiH species; $\Delta\mu^E_{LiH} = -RT \ln (x_{LiH} + {}^1/_2 x_{LiCl})$.

energy of the solution, was expressed as

$$\Delta\bar{G}^E = x_1x_2(a + bx_1 + cx_1^2) \qquad (5)$$

and assumed to be independent of the temperature. The excess chemical potentials then may be expressed as

$$\Delta\mu^E_1 = x_2^2(a + 2bx_1 + 3cx_1^2) \qquad (6)$$

$$\Delta\mu^E_2 = x_1^2(a - b + 2(b - c)x_1 + 3cx_1^2) \qquad (7)$$

These equations must satisfy the Gibbs–Duhem equation within the assumption that the coefficients are independent of the temperature. The values of the excess chemical potentials of both components were then smoothed as a function of x_1 simultaneously by a least-squares method with the use of eq. 6 and 7. The values of the coefficients obtained are: $a = 1882$, $b = -1831$, $c = 2462$. These data are given in Fig. 4, where the excess chemical potential for each component is given as a function of composition. The circles are the experimental data points and the lines represent the least-squares calculation for the function $\Delta\mu^E_i$; the lines are extrapolated into the region where experimental verification was not possible. The agreement with the observed values is believed to be satisfactory within the assumptions that have been made. It is not possible to separate any apparent thermodynamic inconsistency from possible temperature effects.

The unusual behavior of $\Delta\mu^E_{LiCl}$ in the region of the eutectic again points up the peculiarities encountered for the various thermodynamic functions in this area of the phase diagram. The data for the lithium chloride side show a definite change in slope as one approaches the eutectic. This is not quite as apparent on the lithium hydride side, although marked deviations are observed if one should include the eutectic composition in the calculations. As yet, experimental verification of peritectic formation or some similar phenomena which might explain this behavior has not been found.

The deviations from ideality are positive and quite large. Such positive deviations are usually caused by dispersion forces or association of one of the components. Other factors which have been considered lead to negative deviations.[13] If it is assumed that lithium chloride is a dimeric species Li_2Cl_2 in very dilute solutions in lithium hydride and that the solution is ideal in terms of the species LiH and Li_2Cl_2, the limiting value of the curve of temperature *vs.* composition would be the line $\nu = {}^1/_2$ in Fig. 2. The limiting value of the same function for an ideal solution of LiCl (un-ionized) in lithium hydride, or of Li_2Cl^+ and Cl^- in lithium hydride, would follow the line marked $\nu = 1$. The fact that the experimental data approach the line of $\nu = {}^1/_2$ indicates that LiCl may exist as a dimeric species in dilute solutions in lithium hydride.

A study of the species present in the more concentrated range is illustrated in Fig. 5. The line represents the calculated values of $\Delta\mu^E_{LiH}$ on the basis of ideal solutions formed by the species Li_2Cl_2 and LiH. The points are the observed values (Table I). It is interesting to note how close the experimental values follow the calculated line even up to a mole fraction of LiCl of 0.7.

(13) M. Blander, "Molten Salt Chemistry," Interscience Publishers, New York, N. Y., 1964, pp. 127–237.

This observation gives strong evidence that the species Li_2Cl_2 may exist in these solutions, but it must be realized that the solutions are not ideal and effects such as those due to dispersion and volume must be present.

When lithium hydride is dissolved in lithium chloride the limiting value of a curve of temperature *vs.* composition approaches a value of $\nu = 1$ in Fig. 2. For an ideal solution of LiH (un-ionized) in lithium chloride or Li^+ and H^- in lithium chloride the limiting value of this function would follow a line of $\nu = 1$. Because of the common ion effect one cannot, therefore, distinguish between ionized and un-ionized lithium hydride in this system. There is certainly strong indication from these data that dimerization of the LiH in lithium chloride does not occur.

Of interest to the present discussion are the data of Berkowitz and Chupka[14] on the mass spectrometric examination of the alkali metal halides. They found, for example, that lithium chloride has a dimer:monomer ratio of 2.50:1 for species present in the vapor phase when this vapor is in equilibrium with its condensed phase. Their data show polymerization to be a general characteristic of the lithium salts. The sodium, potassium, and rubidium salts all tend to have monomers as the predominant species present in the vapor phase.

(14) J. Berkowitz and W. A. Chupka, *J. Chem. Phys.*, **29**, 653 (1958).

CONTRIBUTION FROM THE CHEMISTRY DEPARTMENT,
BROOKHAVEN NATIONAL LABORATORY, UPTON, NEW YORK 11973

Crystal and Molecular Structure of Manganese Pentacarbonyl Hydride[1]

BY SAM J. LA PLACA, WALTER C. HAMILTON, AND JAMES A. IBERS

Received June 22, 1964

Manganese pentacarbonyl hydride, $HMn(CO)_5$, crystallizes with eight molecules in space group I2/a of the monoclinic system in a cell which at $-75°$ has the dimensions $a = 12.18$, $b = 6.35$, $c = 19.20$ Å., and $\beta = 93.3°$. Three-dimensional X-ray data were collected from crystals grown from the liquid phase, and the structure was solved by standard techniques. Although the H atom was not located, its profound influence on the geometry of the molecule can be inferred from the fact that the $Mn(CO)_5$ portion of the molecule shows insignificant deviations from C_{4v} symmetry: the five carbon atoms of the carbonyls occupy five of the six corners of a nearly regular octahedron; the manganese atom lies slightly above the basal plane along the fourfold axis toward the apical carbonyl group. This result is in direct contrast to claims from infrared studies that the molecule in the gas phase definitely has symmetry lower than C_{4v}, and to arguments based on the marked similarities in chemical and physical properties of $HMn(CO)_5$ and $Fe(CO)_5$ that $HMn(CO)_5$ must be a trigonal bipyramid with the H buried in the metal orbitals.

Introduction

Based in part on chemical and physical studies of transition metal carbonyl hydrides by Hieber and his associates[2] and in part on spectroscopic and theoretical studies by Cotton and his associates,[3-5] the notion has developed that the metal–hydrogen bond in transition metal carbonyl hydrides is abnormally short and that the hydrogen exerts little, if any, influence on the geometrical arrangement of the other ligands around the metal. Thus Hieber and Wagner[2] describe the Mn–H group as a pseudo-Fe atom, and Cotton and Wilkinson[3] suggest that the proton is buried in the electron density of the metal atom. In the past few years there has accumulated evidence from diffraction studies, evidence more direct than that based on spectroscopic data and physical properties, that the hydrogen atom is at a normal distance from the metal and in fact exerts a profound influence on the geometrical arrangement of other ligands about the metal in partially and totally substituted transition metal carbonyl hydrides. For example, Owston, Partridge, and Rowe[6] showed that the phosphorus and bromine atoms in $HPt[P(C_2H_5)_3]_2Br$ were at three of the four corners of a square, with the platinum at the center.[7] Similarly, Orioli and Vaska[8] found that in $HOsBr(CO)[P(C_6H_5)_3]_3$ the bromine, carbon, and three phosphorus atoms were at five of the six vertices of an octahedron. More recently, La Placa and Ibers[9,10] not only found that in $HRh(CO)[P(C_6H_5)_3]_3$ the carbon and three phosphorus atoms were at four of the five vertices of a trigonal bipyramid, as might be expected on the basis of the earlier studies that showed the influence of hydrogen on the geometry, but they also located the hydrogen itself at the fifth vertex at a normal covalent Rh–H distance of 1.60 ± 0.12 Å.

Still the argument might be made[11] that these substituted carbonyl hydrides differ from the parent compounds on which most of the spectroscopic data have been collected. This seems unlikely in view of the

(1) Research performed under the auspices of the U. S. Atomic Energy Commission.
(2) W. Hieber and G. Wagner, *Z. Naturforsch.*, **13b**, 340 (1958).
(3) F. A. Cotton and G. Wilkinson, *Chem. Ind.* (London), 1305 (1956).
(4) F. A. Cotton, J. L. Down, and G. Wilkinson, *J. Chem. Soc.*, 833 (1959).
(5) F. A. Cotton, *J. Am. Chem. Soc.*, **80**, 4425 (1958).
(6) P. G. Owston, J. M. Partridge, and J. M. Rowe, *Acta Cryst.*, **13**, 246 (1960).
(7) Similar results have been obtained by R. Eisenberg and J. A. Ibers (unpublished) on $HPt[PC_2H_5(C_6H_5)_2]_2Cl$.
(8) P. L. Orioli and L. Vaska, *Proc. Chem. Soc.*, 333 (1962).
(9) S. J. La Placa and J. A. Ibers, *J. Am. Chem. Soc.*, **85**, 3501 (1963).
(10) S. J. La Placa and J. A. Ibers, *Acta Cryst.*, in press.
(11) J. Chatt, *Proc. Chem. Soc.*, 318 (1962).